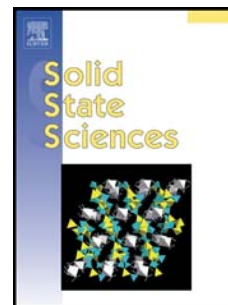


Accepted Manuscript

Synthesis of silanized maghemite nanoparticles onto reduced graphene sheets composites

C. Cosio-Castañeda, R. Martínez-García, L.M. Socolovsky



PII: S1293-2558(14)00026-0

DOI: [10.1016/j.solidstatesciences.2014.02.004](https://doi.org/10.1016/j.solidstatesciences.2014.02.004)

Reference: SSSCIE 4888

To appear in: *Solid State Sciences*

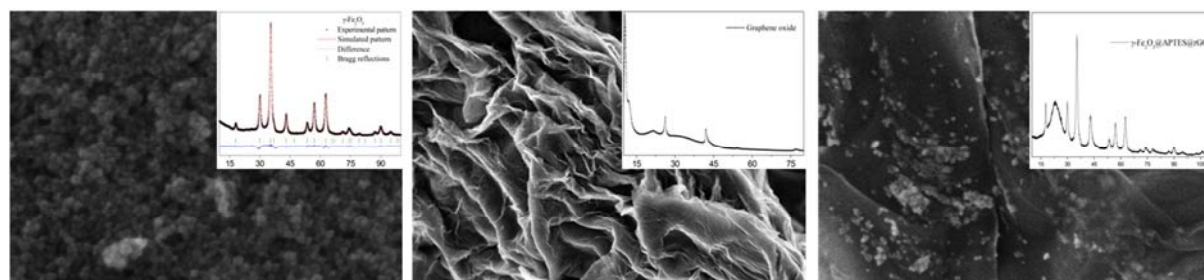
Received Date: 22 May 2013

Revised Date: 22 November 2013

Accepted Date: 3 February 2014

Please cite this article as: C. Cosio-Castañeda, R. Martínez-García, L.M. Socolovsky, Synthesis of silanized maghemite nanoparticles onto reduced graphene sheets composites, *Solid State Sciences* (2014), doi: 10.1016/j.solidstatesciences.2014.02.004.

This is a PDF file of an unedited manuscript that has been accepted for publication. As a service to our customers we are providing this early version of the manuscript. The manuscript will undergo copyediting, typesetting, and review of the resulting proof before it is published in its final form. Please note that during the production process errors may be discovered which could affect the content, and all legal disclaimers that apply to the journal pertain.



SYNTHESIS OF SILANIZED MAGHEMITE NANOPARTICLES ONTO REDUCED GRAPHENE SHEETS COMPOSITES

C. Cosio-Castañeda^{a,b,*}, R. Martínez-García^a, L.M. Socolovsky^a

^aLaboratorio de Sólidos Amorfos, INTECIN, Facultad de Ingeniería, Universidad de Buenos Aires, C1063ACV, Buenos Aires, Argentina.

^bDepartamento de Física y Química Teórica, Facultad de Química, Universidad Nacional Autónoma de México, Ciudad Universitaria, D.F. 04510, México.

*corresponding author: carloscosioc@gmail.com.

Address: Paseo Colón 850, Ciudad Autónoma de Buenos Aires, C1063ACV, Argentina.

Telephone/fax: 0054911 4343-0893/0092, int. 232.

Abstract

Novel $\gamma\text{-Fe}_2\text{O}_3\text{@APTES@rGO}$ composites are successfully synthesized by using graphene oxide and silanized maghemite nanoparticles. Graphene oxide and maghemite were obtained by Hummers and Massart methods, respectively. The silanization process was done to functionalize maghemite surface with a controllable quantity of amino groups. Then, by adding aqueous graphene oxide suspension, the bonding between graphene oxide and silanized maghemite nanoparticles was done in refluxing conditions. Afterwards, chemical reduced graphene oxide reaction was realized by addition of hydrazine solution. The characterization of $\gamma\text{-Fe}_2\text{O}_3\text{@APTES@rGO}$ composites was studied by X-ray Diffraction, Fourier Transformed Infrared Spectroscopy, thermogravimetric analysis and scanning electron microscopy.

KEYWORDS: Maghemite, APTES, Graphene, surface density, composite.

1- Introduction

The development of nanocomposite systems formed by nanostructured materials with their own chemical and physical properties is a growing research area in nanotechnology because of their potential technological applications in biosensors[1], supercapacitors[2], and other nanodevices[3]. Recently, graphene has been the focus of much research given their unique structural, electrical, thermal and mechanical properties [4-10]. Graphene shows magnetoresistive properties linked to its organic nature, that can be used as a base for a magnetoresistive device [11,12]. Granular materials composed by magnetic nanoparticles dispersed in a matrix displays giant magnetoresistance, which is originated in a different physical property, the orientation of the magnetic supermoments of the superparamagnetic nanoparticles [13, 14]. Therefore, an interesting system can be prepared by attaching magnetic nanoparticles to molecular organic materials, particularly graphene layers [15, 17]. Maghemite nanoparticles ($\gamma\text{-Fe}_2\text{O}_3$) are commonly used due to their intrinsic stability against oxidation, and large specific magnetization [18,19]. This letter reports preparation and characterization of composites formed by $\gamma\text{-Fe}_2\text{O}_3$ nanoparticles, functionalized with aminopropyltriethoxysilane (APTES). This process is used to anchor nanoparticles to other molecular structures [20-23]. After this functionalization, the obtained structure $\gamma\text{-Fe}_2\text{O}_3\text{@APTES}$ is attached to reduced graphene oxide layers (rGO), named now $\gamma\text{-Fe}_2\text{O}_3\text{@APTES@rGO}$. In a former article, Il T. Kim *et. al.* obtained a new compound where graphene was decorated with $\gamma\text{-Fe}_2\text{O}_3$ nanoparticles [17]. However, the main difference between the compound synthesized by Il T. Kim *et. al.* and the

ACCEPTED MANUSCRIPT

composite reported here is the presence of the propylsilane linking graphene with $\gamma\text{-Fe}_2\text{O}_3$ nanoparticles. Such differences result in a quantitative control of the association between nanoparticles and graphene (the components of composite). The synthesis process is resumed as 1) silanizing $\gamma\text{-Fe}_2\text{O}_3$ with 3-aminopropyltriethoxysilane (APTES); 2) coupling between $\gamma\text{-Fe}_2\text{O}_3\text{@APTES}$ compounds and graphene oxide (GO); and 3) chemical reduction of graphene oxide preserving the $\gamma\text{-Fe}_2\text{O}_3$ silane-coating and its bonding to the graphene sheet. The experimental results show that chemically reduced graphene oxide sheets (rGO) are linked to $\gamma\text{-Fe}_2\text{O}_3\text{@APTES}$ nanoparticles.

2- Materials and methods

Preparation of maghemite nanoparticles: $\gamma\text{-Fe}_2\text{O}_3$ nanoparticles has been synthesized by a modified Massart procedure [24]. An aqueous mixture of FeCl_3 and $\text{Fe}(\text{NH}_4)_2(\text{SO}_4)_2$ (molar ratio 2:1) is co-precipitated with concentrated NH_4OH . After one hour of reaction, the precipitate is filtered and washed with distilled water until pH 7. The obtained product, composed by magnetite nanoparticles (Fe_3O_4) is dispersed into an acidic solution of HNO_3 and $\text{Fe}(\text{NO}_3)_3$ (pH 2 and ionic strength of 14.6 mM) at 80°C . The oxidation of Fe_3O_4 to $\gamma\text{-Fe}_2\text{O}_3$ occurred under vigorous stirring for 4 h. Finally, the supernatant is removed and the solid resultant powder is washed with acetone.

Silanized maghemite nanoparticles: 250 mg of $\gamma\text{-Fe}_2\text{O}_3$ nanoparticles were dispersed in ethanol (200 ml), then dispersion was mixed with APTES in a molar ratio of 1:1 ($\gamma\text{-Fe}_2\text{O}_3\text{@APTES}^1$) and 1:10 ($\gamma\text{-Fe}_2\text{O}_3\text{@APTES}^{10}$). The solution was kept for seven hours in refluxing conditions. Solid products ($\gamma\text{-Fe}_2\text{O}_3\text{@APTES}$) were centrifuged and dried at 80°C .

Graphene oxide synthesis: GO was synthesized using Hummers method [25]. Synthetic graphite (2 g, 100 mesh) was added to concentrated H_2SO_4 (46 ml) and stirred at 0°C for 24 h. Afterwards, NaNO_3 (200 mg) was added to the mixture while keeping temperature and stirring. For oxidation, KMnO_4 (6 g) was added slowly keeping temperature below 35°C . Then, water (86 ml) was dropped at a rate of 1.5 ml/min. Finally, water (280 ml) and H_2O_2 (20 ml, 30%) were added to terminate the reaction. The obtained solid was centrifuged, washed with HCl (10 %) and water.

Composite formation: GO (250 mg) was ultrasonicated in NaOH solution (500 ml, pH 10) and stirred for 5 h. Then, $\gamma\text{-Fe}_2\text{O}_3\text{@APTES}$ (50 mg) and dicyclohexylcarbodiimide (2 mg) were added into GO solution and kept in refluxing condition for 24 h. Obtained solid ($\gamma\text{-Fe}_2\text{O}_3\text{@APTES@GO}$) was magnetically separated and dried. The reduction process occurs when $\gamma\text{-Fe}_2\text{O}_3\text{@APTES@GO}$ (50 mg) was suspended in an aqueous hydrazine solution (10 ml, 35%) under stirring and heating (90°C) for 2 h [26]. The final solid ($\gamma\text{-Fe}_2\text{O}_3\text{@APTES@rGO}$) was washed with water to remove hydrazine residual and dried at 60°C .

Characterization

X-ray diffraction (XRD) patterns were collected at room temperature with a Rigaku diffractometer (Cu K_α radiation, $\lambda=1.54056 \text{ \AA}$) in 2θ range from 10° to 110° with scan range of $0.12^\circ/\text{min}$. Fourier transformed infrared

(FT-IR) spectra were recorded with an IRAffinity-1 spectrophotometer, in 4000-500 cm^{-1} range, using standard KBr pellet technique. Thermal stability of compounds was investigated using a TGA-50 Thermogravimetric Analyzer under static air atmosphere at a heating rate of 10 $^{\circ}\text{C min}^{-1}$. Scanning electron microscopy (SEM) images were obtained with a Carl Zeiss Supra 40 field emission SEM microscope. Magnetization was measured in a Quantum Design MPMS SQUID magnetometer.

3- Results and discussion

Figure 1, (a) and (b), show XRD patterns of $\gamma\text{-Fe}_2\text{O}_3\text{@APTES@GO}$ and $\gamma\text{-Fe}_2\text{O}_3\text{@APTES@rGO}$ composites, respectively. As can be seen, the presence of $\gamma\text{-Fe}_2\text{O}_3$ nanocrystalline was confirmed by the characteristic reflections associated with maghemite phase. In Figure 1(a), the peak around 11° is related to GO, but, after hydrazine reduction, this peak vanishes and a poorly ordered graphene signal near to 22° appears, Figure 1(b). The peak of 22° is associated to (002) rGO [27]. In $\gamma\text{-Fe}_2\text{O}_3\text{@APTES@GO}$ XRD patterns, there are three peaks around 26.4° , 44.6° , 77.4° that are assigned to (002), (101), (110) reflections of graphite (PDF 89-8487), respectively. The presence of these peaks can refer to an incomplete graphene conversion. Nevertheless, the existence of graphite impurities does not affect the conversion of GO to rGO.

Magnetization vs applied field measurements of silanized nanoparticles (not shown here) gave a saturation magnetization between 49 and 61 emu/g, compatible with accepted values for maghemite [28, 29], below the bulk saturation value (about 76 emu/g [30]).

In order to confirm silanized $\gamma\text{-Fe}_2\text{O}_3$, FT-IR and TGA measurements were performed. In Figure 2a are shown the characteristic absorption bands of the aminopropyl groups as well as the stretching vibration of Fe–O and Si–O bonds. So, it is inferred that APTES is successfully bonded to $\gamma\text{-Fe}_2\text{O}_3$. In TGA results, two weight-loss stages were observed (Figure 2b). The first one was associated with the loss of H_2O , while the second one is the result from aminopropyl group decomposition. The temperature ranges and weight loss percentages are summarized in Figure 2b inset. Based in second weight-loss stage, it is possible to determinate APTES surface density. For this, molecular formula of $\gamma\text{-Fe}_2\text{O}_3\text{@APTES}$ was considered as $\text{H}_2\text{N}((\text{CH}_2)_3\text{-SiO}_3\text{-(Fe}_2\text{O}_3)_n$, with n as the coated particle ratio. As a result, APTES surface density is 3.69 ($n\sim 8$) and 4.93 ($n\sim 6$) molecules/ nm^2 for $\gamma\text{-Fe}_2\text{O}_3\text{@APTES}^1$ and $\gamma\text{-Fe}_2\text{O}_3\text{@APTES}^{10}$, respectively. Additionally, in Figure 2b is observed that when APTES surface density increase, the decomposition temperature range increases. This could be associated with an increase in thermal stability [31,32].

Moreover, when analyzing the FT-IR spectra associated with $\gamma\text{-Fe}_2\text{O}_3\text{@APTES@rGO}$, Figure 2c, it can be observed the absence of N-H stretching and NH_2 bending mode of amino group as an effect of covalent bonds between $\gamma\text{-Fe}_2\text{O}_3\text{@APTES}$ and GO sheets [33]. In TGA measurements of two composites (Figure 2d) are observed three weight-loss stages that are associated with the loss of H_2O , residual functional groups and rGO sheets, respectively [34, 35]. As can be seen, the rGO loss is higher for the composite which has the largest

number of amino groups in the coating. This effect confirms that there is a direct dependence between the coated characteristics and the amounts of graphene sheets in the synthesized composite.

The morphology and structural features of $\gamma\text{-Fe}_2\text{O}_3\text{@APTES}$, GO sheets and composite were studied by using SEM. Figure 3a shows a SEM image of $\gamma\text{-Fe}_2\text{O}_3\text{@APTES}$ in which is clear that discrete coated-nanoparticles have a spherical shape. As shown in this image, $\gamma\text{-Fe}_2\text{O}_3\text{@APTES}$ are small with a size of about 10 nm, which can become a spacer to prevent a posterior restacking of individual graphene sheets. From the image of GO, Figure 3b, it can be seen that graphene layer are exfoliated to a large extent, with a wrinkled structure that provides a large rough surface as scaffold for further modification. After reaction between $\gamma\text{-Fe}_2\text{O}_3\text{@APTES}$ and GO, and the posterior reduction process with hydrazine, the coated-nanoparticles are completely distributed on rGO sheets (Figure 3c) indicating the composite formation. In this representative SEM image of the composite, the graphene sheets exhibit a slightly wrinkled surface and the coated-nanoparticles appear as bright dots. Many $\gamma\text{-Fe}_2\text{O}_3\text{@APTES}$ spheres are firmly anchored on both sides of the wrinkled graphene sheets. The graphene layers might contribute to hinder coated-nanoparticles aggregation.

4- Conclusion

In summary, we have successfully synthesized a novel nanocomposite based on $\gamma\text{-Fe}_2\text{O}_3\text{@APTES}$ nanoparticles and chemically reduced graphene oxide sheets. The results from XRD, FT-IR and TGA clearly indicate that coated-nanoparticles and graphene sheets are firmly tethered by covalent bonding. However, the graphene oxide quantity present in the composite can be influenced as a function on amount of amino groups that constitute the $\gamma\text{-Fe}_2\text{O}_3$ coating.

5- Acknowledgements

Agencies of Argentina (CONICET and ANPCyT) and Mexico (CONACyT) for financial support. We thank Lorena Maldonado for technical assistance in FT-IR and TGA measurements.

References

- [1] Haun JB, Yoon T-J, Lee H, Weissleder R. WIREs Nanomed Nanobiotechnol 2010; 2:291-304.
- [2] Zhi M, Xiang C, Li J, Li M, Wu N. Nanoscale 2013; 5:72-88.
- [3] Quandt A, Ferrari M. Advances in Science and Technology 2008; 55:74-83.
- [4] Dreyer DR, Park S, Bielawski CW, Ruoff RS. Chem Soc Rev 2010; 39:228-240.
- [5] Castro NAH, Guinea F, Peres NMR, Novoselov KS, Geim AK. Rev Mod Phys 2009; 81:109-162.
- [6] Young RJ, Gong L, Kinloch IA, Riaz I, Jalil R, Novoselov KS. ACS Nano 2011; 5:3079-3084.

[7] Valota AT, Kinloch IA, Novoselov KS, Casiraghi C, Eckmann A, Hill EW, Dryfe RAW. ACS Nano 2011; 5:8809-8815.

[8] Gong L, Young RJ, Kinloch IA, Riaz I, Jalil R, Novoselov KS. ACS Nano 2012; 6:2086-2095.

[9] Huang X, Qi X, Boey F, Zhang H. Chem Soc Rev 2012; 41:666-686.

[10] Sannigrahi J, Bhadra D, Masud MdG, Chaudhuri BK. AIP Conf Proc 2012; 14447:953-954.

[11] Gu H, Zhang X, Wei H, Huang Y, Wei S and Guo Z; Chem. Soc. Rev. 2013; 42:5907-5943

[12] Zhu J, Wei S, Haldolaarachchige N, He J, Young DP and Guo Z. Nanoscale 2012; 4:152–156

[13] Chien CL, Xiao JQ, Jiang JS. J. Appl. Phys. 1992; 73:5309 - 5314

[14] Socolovsky LM, Denardin JC, Brandl AL, Knobel M. Mat. Char. 2003; 50:117 – 121

[15] He Q, Yuan T, Wei S, Haldolaarachchige N, Luo Z, Young DP, Khasanov A, and Guo Z. Angew. Chem. Int. Ed. 2012; 51:8842 – 8845.

[16] Zhu J, Luo Z, Wu S, Haldolaarachchige N, Young DP, Wei S and Guo Z. J. Mater. Chem. 2012; 22:835-844. Zhang X, Alloul A, He Q, Zhu J, Verde MJ, Li Y, Wei S, Guo Z. Polymer 2013; 54:3594 – 3604.

[17] Kim IT, Magasinski A, Jacob K, Yushin G, Tannenbaum R. Carbon 2013; 52:56-64.

[18] Fiorani D, Testa AM, Lucari F, D’Orazio F, Romero H. Physica B 2002; 320:122-126.

[19] Chatterjee J, Haik Y, Chen C-J. J Magn Magn Mater 2003; 257:113-118.

[20] Zhu J, Wei S, Lee IY, Park S, Willis J, Haldolaarachchige N, Young DP, Luo Z and Guo Z. RSC Adv. 2012; 2:1136-1143.

[21] Zhu J, Wei S, Haldolaarachchige N, Young DP, and Guo Z. J. Phys. Chem. C 2011; 115:15304 -15310.

[22] Zhu J, Wei S, Ryu J, Budhathoki M, Liang G, and Guo Z. J. Mat. Chem. 2010; 20:4937 – 4948.

[23] Zhu J, Wei S, Yadav A, Guo Z. Polymer 2010; 51(12):2643-2651.

[24] Massart R. IEEE T Magn 1981; 17:1247-1248.

[25] Hummers WS, Offerman RE. J Am Chem Soc 1958; 80:1339.

[26] Pei S, Cheng HM. Carbon 2012; 50:3210-3228.

[27] Park S, An J, Potts JR, Velamakanni A, Murali S, Ruoff RS. Carbon 2011; 49:3019-3023.

[28] Glaria A, Kahn ML, Falqui A, Lecante P, Collière V, Respaud M, Chaudret B. Chem. Phys. Chem. 2008; 9:2035-2041.

[29] Moscoso-Londoño O, Carrião MS, Cosio-Castañeda C, Bilovol V, Socolovsky LM, Martínez Sánchez R, Lede EJ, Martínez-García R; Mat. Res. Bull. 2013; 48 (9):3474-3478

[30] Handley CO, Modern Magnetic Materials: Principles and Applications, Wiley-Interscience, New York, 2000.

[31] Li Y-S, Church JS, Woodhead AL. J Magn Magn Mater 2012; 324:1543-1550.

[32] Poursaberi T, Hassanisadi M, Torkestani K, Zare M. Chem Eng J 2012; 189-190:117-125.

[33] Shen J, Hu Y, Shi M, Li N, Ma H, Ye M. J Phys Chem C 2010; 114:1498-1503.

[34] Wang G, Liu T, Luo Y, Zhao Y, Ren Z, Bai J, Wang H. J Alloy Comp 2011; 509:L216-L220.

[35] Liu Z, Duan X, Qian G, Zhou X, Yuan W. Nanotechnology 2013; 24:045609.

Figure 1. XRD patterns for (a) $\gamma\text{-Fe}_2\text{O}_3\text{@APTES@GO}$ and (b) $\gamma\text{-Fe}_2\text{O}_3\text{@APTES@rGO}$ composites. In figure 1(a), the diffraction peaks can be assigned to $\gamma\text{-Fe}_2\text{O}_3$, GO(*) and graphite(▪). The inset in (a) shows the structural analysis of $\gamma\text{-Fe}_2\text{O}_3$ from which was obtained the particle size (12.83 nm). In figure 1(b), the diffraction peaks can be associated to $\gamma\text{-Fe}_2\text{O}_3$ and rGO(▼). The inset in (b) shows XRD of graphite, GO and rGO.

Figure 2. FT-IR and TGA measurements for $\gamma\text{-Fe}_2\text{O}_3\text{@APTES}$ and $\gamma\text{-Fe}_2\text{O}_3\text{@APTES@rGO}$ compounds. FT-IR signal assignation, in Figure (a) and (c), was performed with data previously reported in the literature [31-33]. The absorption band associated with the Fe–O–Si bond cannot be seen because it appears near to 580 cm^{-1} and it would overlap with the Fe–O vibrations of $\gamma\text{-Fe}_2\text{O}_3$.

Figure 3. SEM images of (a) $\gamma\text{-Fe}_2\text{O}_3\text{@APTES}$, (b) GO sheets and (c) $\gamma\text{-Fe}_2\text{O}_3\text{@APTES@rGO}$ composite.

Figure 1.

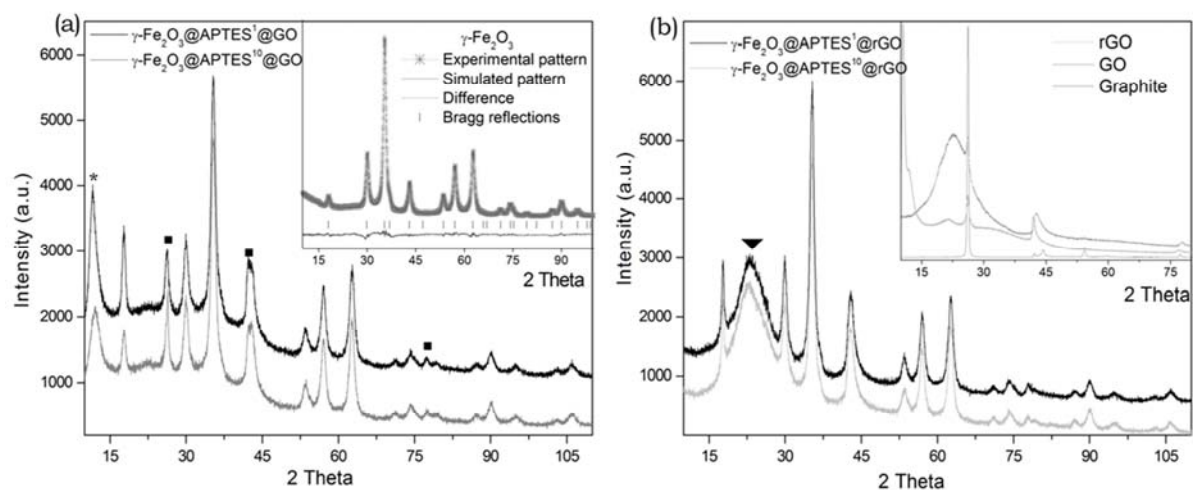
ACCEPTED MANUSCRIPT

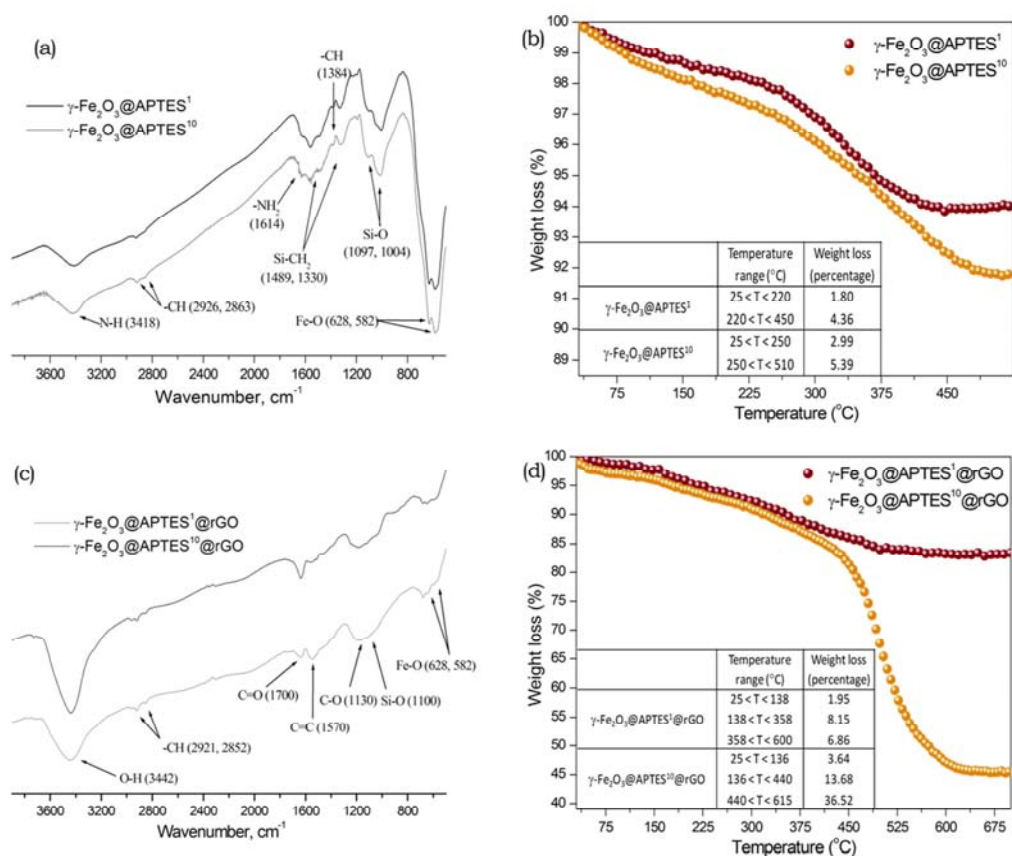
Figure 2.

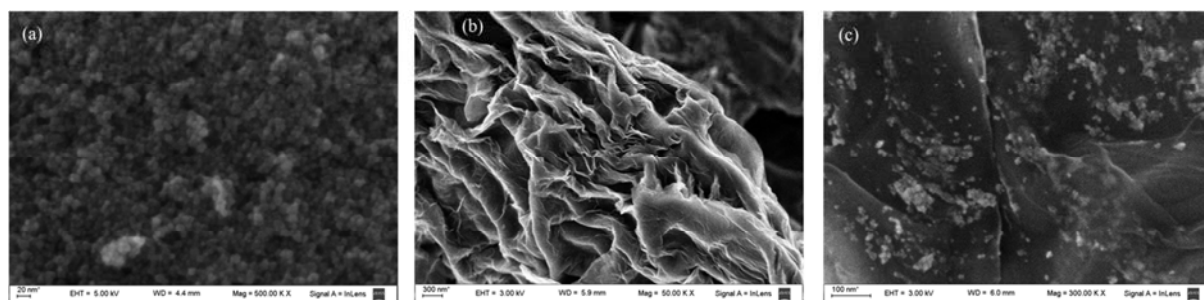
ACCEPTED MANUSCRIPT

Figure 3.

ACCEPTED MANUSCRIPT







- Novel $\gamma\text{-Fe}_2\text{O}_3\text{@APTES@rGO}$ composites are synthesized.

- Silanization process of maghemite nanoparticles was done in controllable quantity.
- XRD, FT-IR, TGA and SEM techniques were used to confirm the composite existence.